Science of Sintering, **46** (2014) 129-134

doi: 10.2298/SOS1401129J

UDK 535.37

The Luminescent Properties of Yttrium Oxyapatite Doped with Eu^{3+} ions

V. Jokanović[1*)], B. Čolović[1], N. Jović[1]

[1]Vinča Institute of Nuclear Sciences, University of Belgrade,
Mike Petrovica Alasa 12-14, Belgrade, Serbia

Abstract:

The structural and luminescent properties of $Ca_2Y_8(SiO_4)_6O_2$ (CYS) silicate based oxyapatite doped with Eu^{3+} ions have been reported in this paper. The sample was synthesized using reflux method assisted by urea subsequent degradation. Very specific, shell- and rope-like morphologies were observed by SEM. The powder X-ray diffraction study revealed that the Eu^{3+}: CYS system crystallized in a hexagonal lattice structure (space group P63/m) characteristic of oxyapatite. In the host oxyapatite structure, a partial replacement of Ca^{2+} and Y^{3+} ions by luminescent active Eu^{3+} ions have been done, and its photoluminescent spectra were analyzed. The performed analysis indicate the presence of Eu^{3+} ions in both, nine-fold coordinated 4f, and seven-fold coordinated 6h sites, showing a slight shift towards the blue area in comparison to a typical spectra of other yttrium-silicate phases as hosts.

Keywords: *Urea assisted reflux method, Europium doped yttrium oxyapatites, Luminescent properties, Crystal structure.*

1. Introduction

Recently, luminescent materials have attracted great attention because of their potential application in high-resolution devices such as: cathode ray tubes (CRTs), flat panel display devices, or field emission displays (FEDs) [1, 2]. In the past decade, the sol–gel method became one of the most attractive methods for synthesis of various luminescent ceramics composed of different host materials in which rare earth metal ions have been incorporated, e.g. Y_2SiO_5:Tb and $Y_3Al_5O_{12}$:Tb systems for cathodoluminescence, $Y_3Al_5O_{12}$:Eu and $Y_3(Al, Ga)_5O_{12}$:Tb for field emission displays, Y_2O_3:Eu, TiO_2:Eu and Zn_2SiO_4:Mn/Tb for photoluminescence, and ZnS:Mn/Tb and Ga_2O_3:Eu/Mn for electroluminescence [3-5]. Recently, solvothermal and hydrothermal methods are particularly investigated because they enable synthesis of the luminescent materials of very interesting morphology [6].

A special attention among the host materials belongs to the $Ca_2RE_8(SiO_4)_6O_2$ (RE is Y, Gd or La) oxyapatite, which can be used to host various luminescence active rare earth ions [7-12]. The most prominent structural characteristic of oxyapatites is the possibility of rare earth ions to simultaneously occupy two different crystallographic sites, the nine-fold coordinated 4*f* site (with C_3 point symmetry) and the seven-fold coordinated 6*h* site (with C_S point symmetry) in the hexagonal lattice structure (space group *P*63/*m*). In this paper, the structural and luminescent properties of low-temperature synthesized $Ca_2Y_8(SiO_4)_6O_2$:Eu^{3+}

*) **Corresponding author**: vukoman@vinca. rs

system, obtained by urea assisted sol-gel method, have been studied. Taking in mind that conventional processes of oxyapatite synthesis require significantly higher temperatures than 1000 °C and longer thermal treatments to obtain mono-phase system, the modified procedure of synthesis, used in this study, gives numerous advantages, especially from the aspect of particles nanodesign.

2. Experimental

2.1. Synthesis

For the synthesis of calcium yttrium oxyapatite of chemical formula $Ca_2Y_8(SiO_4)_6O_2$, doped with 1.42 at% of Eu^{3+}, silica sol, calcium, yttrium and europium nitrate salts were mixed in the corresponding stoichiometric ratio. The silica sol is prepared by method described in ref. [13], and an average size of SiO_2 particles was estimated to be 6.7 nm. The synthesis was performed using reflux method, at water boiling temperature during 4 h. The pH value of precursor was adjusted to 9 by adding urea, which brings to an increase of the pH value to the level required for complete hydrolysis of metal ions. After precipitation, the sample was rinsed with deionized water, and then the precipitate was annealed at 800 °C for 4 h. The white powder was obtained.

2.2. Characterizations

The powder X-ray diffraction (XRD) method was used for the phase analysis of such obtained powder, as well as for the estimation of the average crystallite size value and the lattice parameters. Diffraction pattern was collected on a Philips 1710 diffractometer equipped with Cu $K_{\alpha 12}$ radiation. The data were collected in the 2θ range from 9 to 70° with a scanning step of 0.05°, and exposition time of 5 sec per step. The average crystallite size of Eu^{3+}-doped calcium yttrium oxyapatite was determined from the line broadening of (002) reflection using Scherrer equation: $d = K\lambda/B\cos\theta$, where d - is the average diameter of the crystallites (in nm), K – is the shape factor (0.9), B – is the full width at half maximum of reflection, λ – is the wavelength of the employed X-rays and θ is the Bragg diffraction angle.

The specific surface area of powder was estimated using the nitrogen gas absorption BET method (Sorptomatic 1990, Termoquest CE Instruments). 0.20 g of the sample was thoroughly degassed for 3 h at 150 °C, and than the absorption measurement was performed. Under assumption that the synthesized particles are spherical in shape, the average diameter of the particles was estimated using equation: $d_{ebt} = 6/\rho S_w$, where S_w - is the specific surface area, and ρ - is the density of the $Ca_2Y_8(SiO_4)_6O_2$ oxyapatite powders (we used theoretical value, $\rho = 4.2$ g/cm^3).

The morphology and agglomerate size distribution of the powder were observed by scanning electron microscopy (SEM, JEOL JSM-5300).

Photoluminescence properties of $Ca_2Y_8(SiO_4)_6O_2$:Eu^{3+} powder were studied by Perkin Elmer LS45 luminescence spectrometer, equipped with the excitation source (an optical parametric oscillator (OPO) pumped by the third harmonic of the Nd:YAG laser). The emission was analyzed using HR250 monochromator (Jobin–Yvon). The data was collected using an ICCD camera (Princeton Instrument). In order to limit the contribution of the $^5D_1$ emission, the photoluminescence spectra were obtained with 1 ms time delay after the laser pulse. The emission spectra were recorded after excitation into the strongest $^7F_0 \rightarrow {}^5D_2$ absorption band.

3. Results

3.1. XRD study

Fig. 1 shows the XRD patterns of $Ca_2Y_{8-x}Eu_x(SiO_4)_6O_2$ (x=0.0142) oxyapatite powder after thermal treatment at 800 °C. Pretty narrow diffraction peaks pointed out on a well crystallized grains and low density of strains inside crystal structure. As $Ca_2Y_8(SiO_4)_6O_2$ is isostructural with natural oxyapatite phase $Ca_{10}(PO_4)_6F_2$, all reflections were indexed in the space group (*S.G.*) *P*63/*m*, as follow: 22.1° (200), 23.3° (111), 26.3° (002), 28.7° (120), 29.2° (102), 32.2° (121), 32.8° (112), 33.3° (300), 47.4° (222), 48.8° (213), 50.3° (123), 51.9° (402), and 52.6° (004) (in agreement with JCPDS Card 27-93). The experimental XRD patterns were analyzed by *FullProf* program in a full profile-matching mode (Fig.1). The refined lattice parameters were found to be: $a = b = 9.360(1)$ Å, $c = 6.790(1)$ Å. The average crystallite size obtained using Sherrer equation was found to be about 45 nm.

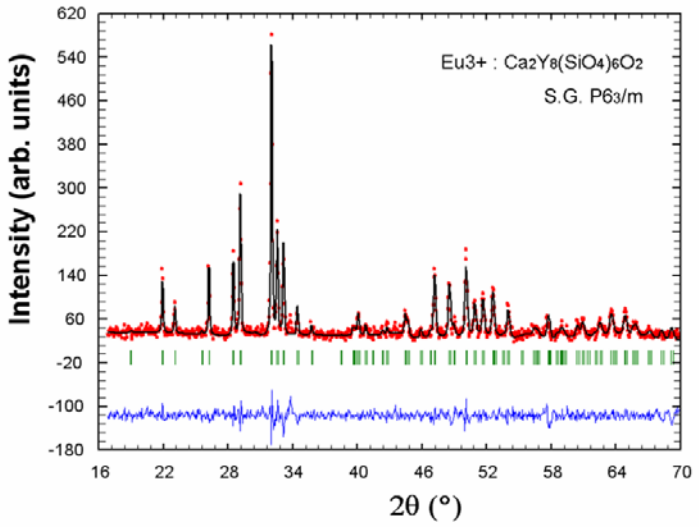

Fig. 1. Experimental (dots) and refined (line) XRD diffraction pattern of $Ca_2Y_8(SiO_4)_6O_2:Eu^{3+}$ powder annealed at 800 °C.

3.2. SEM and BET investigations

The SEM images of $Ca_2Y_8(SiO_4)_6O_2:Eu^{3+}$ powder, shown in Fig. 2, give insight into a morphology of the powder. As it can be seen, particles are agglomerated and form aggregates of shell- and rope-like shape.

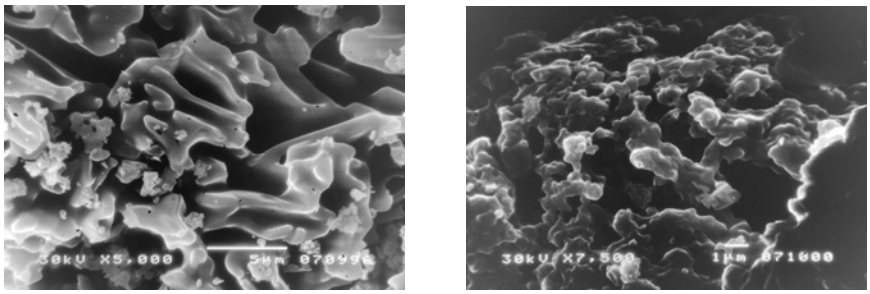

a) b)

Fig. 2. Typical morphology of $Ca_2Y_8(SiO_4)_6O_2:Eu^{3+}$ particles; a) shell-like platelets; and b) rope-like rings.

The platelet size of shells is up to 5 μm, with small broken pieces in between, less than 1 μm in size (Fig. 2a). On the other side, the rope-like agglomerates (Fig.2b) are consisted of spherical particles less than 1 μm in size which are probably built of assembly of even smaller particles. The particles size value obtained by BET analysis was found to be ~55 nm, and is very close to the average crystallite size obtained by XRD analysis (~45 nm).

3.3. Photoluminescence properties

The fluorescence spectra of Eu^{3+}-doped $Ca_2Y_8(SiO_4)_6O_2$, excited by 476.5 nm wavelength, is shown on the Fig 3a.

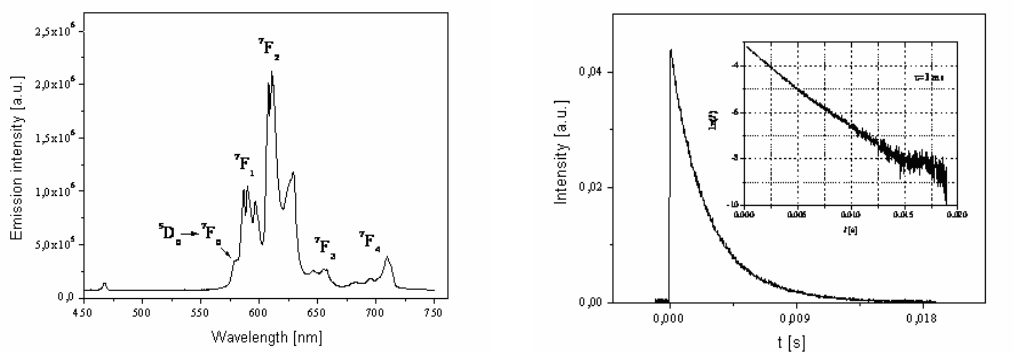

a) b)

Fig. 3. Emission spectra of $Ca_2Y_8(SiO_4)_6O_2:Eu^{3+}$: a) typical emission bands; b) $^5D_0$ decay profile lifetime line at room temperature. Estimated lifetime is 3 ms.

The fluorescence spectrum of $Ca_2Y_8(SiO_4)_6O_2:Eu^{3+}$ oxyapatite, obtained upon excitation at 396 nm (Fig.3a), shows all characteristic emissions lines for Eu^{3+} ions which correspond to the transition lines $^5D_0$-^7F_J (J=0, 1, 2, 3, 4). The emissions from higher ^5D_J (J>O) levels have not been observed, which can be ascribed to the fact that the energy gaps between $^5D_2$ and $^5D_1$, as well as between $^5D_1$ and $^5D_0$ levels of Eu^{3+}, which are 2500 cm^{-1} and 1750 cm^{-1} respectively, silicate groups (with v_{max} = 950 cm^{-1}) are able to bridge, thus joining the gaps between the higher lying levels of the Eu^{3+} ion and the $^5D_0$ level. The most prominent $^5D_0$ -$^7F_2$ emission of Eu^{3+} ions belongs to the hypersensitive, forced electric dipole transition, which is highly sensitive on the symmetry of Eu^{3+} surrounding [1-2]. Generally, the ^7F_J energy levels of free Eu^{3+} ions ($4f^6$ electron configuration) in a crystal lattice split under the effect of crystal field depending on the symmetry of Eu^{3+} site and the number J. In hexagonal oxyapatite structure, the crystal fields with C_3 and C_S symmetry cause splitting of both $^5D_0$-$^7F_1$ and $^5D_0$-$^7F_2$ levels into 3 lines, respectively. $^5D_0$-$^7F_0$ emission line can not be split because J=0. So the number of $^5D_0$-$^7F_0$ lines can be an indication of the number of different Eu^{3+} luminescent centers. It is well known that two $^5D_0$-$^7F_0$ lines indicate that the Eu^{3+} ions probably simultaneously occupy two different sites in the host oxyapatite lattices, e.g. 4*f* (C_3) sites and 6*h* (C_S) sites [7]. The explanation for such prediction can be as follows. The nine-fold coordinated 4*f* site can accommodate larger cations (bigger space), while the seven-fold coordinated 6*h* site is favorable for higher charge cations due to the fact that a cation in this site is surrounding by one free oxygen O(4) ion. The Eu^{3+} has larger effective ionic radii than Y^{3+} (0.120 and 1.075 nm for nine-coordinated Eu^{3+} and Y^{3+} ions, respectively) and higher charge (+3), which are favorable for 4*f* site and 6*h* site, respectively. The competition of these two tendency cause simultaneous occupation of both, 4*f* and 6*h* sites by Eu^{3+} ions. The 4*f* site has no free oxygen ion in its surrounding, while the 6*h* site has one (at a very short distance). Consequently, the seven-fold coordinated Eu^{3+} ions (6*h*) are expected to be more covalently bonded than the nine-fold coordinated Eu^{3+} (4*f*). Therefore, the $^5D_0$-$^7F_0$ emission line at the

lower energy is assigned to Eu^{3+} ions in 6*h* site, and second at higher energy to Eu^{3+} (4*f*) site. It is obvious that the $^5D_0$-$^7F_0$ line of Eu^{3+} (4*f*) is significantly broader than the $^5D_0$-$^7F_0$ transition line of Eu^{3+} (6*h*). This is because the crystal field at the 4*f* site varies, giving rise to an inhomogeneous broadening of the spectral lines. On the contrary, the $^5D_0$-$^7F_0$ transition line of Eu^{3+} (6*h*) is very narrow, because the 6*h* sites exclusively belong to Y^{3+}.

The 4*f* sites and 6*h* sites alternate in the host lattices, i.e. 4*f* (Ca^{2+}, Y^{3+}) - 6*h* (Y^{3+}). So it can be expected the formation of Eu^{3+}(4*f*)-O^{2-}-Y^{3+}(6*h*) and Eu^{3+}(6*h*)-O^{2-}- Ca^{2+} (4*f*) in the host lattices. The next neighbor of Eu^{3+} (4*f*)-0^{2-} is Y^{3+}, so the energy position of Eu^{3+} (4*f*) $^5D_0$-$^7F_0$ is almost similar. As far as Eu^{3+} (6*h*)-O^{2-} is concerned, its next neighbor is Ca^{2+} ion which will influence the degree of covalence of Eu^{3+}(6*h*)-O^{2-} bond. This causes increased degree of covalence of Eu^{3+} (6*h*)-O^{2-} bond making a red shift for Eu^{3+} (6*h*) $^5D_0$-$^7F_0$.

Fig. 3b shows the fluorescence decay curves of the $^5D_0$ emitting level obtained when the sample was excitated at 590 nm (λ_{em} = 613 nm). The fluorescence decay profiles can be adjusted by a single-exponential function in the longer times, while a non-exponential part is observed for the shorter time. The lifetime estimated from this curve is found to be 3 ms, what is quite high value for europium species with low non-radiative energy transfer probability. This fact makes this material very promising from the aspect of optoelectronic applications.

4. Conclusions

In this paper we revealed synthesis procedure, as well as structural and luminescent properties of Eu^{3+}-doped $Ca_2Y_8(SiO_4)_6O_2$ oxyapatite. The sample is obtained from the precipitate synthesized via urea assisted reflux method at pH = 9, which subsequently underwent annealing at 800 °C in air. The XRD analysis confirmed high purity of the sample, giving rise to the high advantages of this over other methods of synthesis. An oxyapatite structure is obtained at significantly lower temperature (about 500 °C), comparing a classical solid state reaction. The average crystallite size was found to be 45 nm (XRD), what is in comparison with the average particle size obtained by BET method (~55 nm). $Ca_2Y_8(SiO_4)_6O_2$:Eu^{3+} nanoparticles aggregate into bigger, spherical particles, 1 μm in size, which further form shell- and rope-like agglomerates order of 1 to 5 μm. The photoluminescence spectra analysis indicate that Eu^{3+} ions simultaneously occupied two different sites inside host calcium yttrium oxyapatite lattices, 4*f* and 6*h* sites (*S.G. P*63/*m*), causing splitting of both $^5D_0$-$^7F_1$ and $^5D_0$-$^7F_2$ emission levels of Eu^{3+} ions into 3 lines, respectively.

Acknowledgement

The Ministry of Education, Science and Technological Development of the Republic Serbia financially supported this work through the project No. 142066.

5. References

1. P. Dorenbos, The Eu^{3+} charge transfer energy and the relation with the band gap of compounds, Journal of Luminescence 111 (2005) 89–104.
2. C. C. Silva, F. P. Filho, A. S. B. Sombra, I. L. V. Rosa, E. R. Leite, E. Longo, J. A. Varela, Study of Structural and Photoluminescent Properties of $Ca_8Eu_2(PO_4)_6O_2$, Journal of Luminescence 18 (2008) 253–259.

3. M. Yu, J. Lin, Y. H. Zhou, S. B. Wang and H. J. Zhang, Sol–gel deposition and luminescent properties of oxyapatite $Ca_2(Y,Gd)_8(SiO_4)_6O_2$ phosphor films doped with rare earth and lead ions, Journal of Materials. Chemistry 12, (2002), 86–91.
4. M. Yu, J. Lin, S.B. Wang, Sol–gel derived silicate oxyapatite phosphor films doped with rare earth ions, Journal of Alloys and Compounds 344 (2002) 212–216.
5. M. Pošarac, A. Devečerski, T. Volkov-Husović, B. Matović, D.M. Dinić, The effect of Y2O3 addition on thermal shock behavior of magnesium aluminate spinel, Science of Sintering 41 (2009) 75-81.
6. G. Seeta Rama Raju, Yeong Hwan Ko, E. Pavitra, and Jae Su Yu, Formation of Ca2Gd8(SiO4)6O2 Nanorod Bundles Based on Crystal Splitting by Mixed Solvothermal and Hydrothermal Reaction Methods, Cryst. Growth Des. 12 (2012) 960−969.
7. Jun Lin and Qiang Su, A study of site occupation of Eu^{3+} in Me, $Y,(Si0_4)_60$, (Me=Mg, Ca, Sr), Materials Chemistry and Physics 38 (1994) 98-101.
8. B. R Jovanić, M. Dramićanin., B. Vianna, B. Panić., B. Radenković, High-pressure optical studies of $Y_2O_3:Eu^{3+}$ nanoparticles, Radiation Effects and defects in Solids, 163, (2008), 925-931.
9. V. Jokanović, M. D. Dramićanin, Ž. Andrić, T. Dramićanin, M. Plavšić, S. Pašalić, M. Miljković, Nanostructure designed powders of optical active materials Me_xSiO_y obtained by ultrasonic spray pyrolysis, Optical Materials 30 (2008) 1168-1172 **.**
10. Ž. Andrić, M. D. Dramićanin, M. Mitrić, V. Jokanović, A. Bessière, B. Viana, Polymer complex solution synthesis of $(Y_xGd_{1-x})_2O_3:Eu^{3+}$ nanopowders, Optical Materials 30 (2008), 1023-1027.
11. M. D. Dramićanin, V. Jokanović, B. Viana, E. Antic-Fidancev, M. Mitrić, Ž. Andrić, Luminescence and structural properties of $Gd_2SiO_5:Eu^{3+}$ nanophosphors synthesized from the hydrothermal obtained silica sol**,** Journal of Alloys and Compounds 424 (2006), 213-217.
12. J. Parmentier, K. Liddell, D. P. Thompson, H. Lemercier, N. Schneider, S. Hampshire, P. R. Bodart, R. K. Harris, Influence of iron on the synthesis and stability of yttrium silicate apatite, Solid State Sciences 3 (2001) 495–502.
13. V. Jokanović, M.D. Dramićanin, Ž. Andrić, B. Jokanović, Z. Nedić, A.M. Spasic Luminescence properties of $SiO_2:Eu^{3+}$ nanopowders: Multi-step nano-designing Journal of Alloys and Compounds, 453, 1-2, (2008), 253-260.

Садржај: *Структурне и луминесцентне особине оксиапатита $Ca_2Y_8(SiO_4)_6O_2$ (CYS) допираног Eu^{3+} јонима приказане су у овом раду. Узорак је синтетисан рефлукс методом, уз постепену деградацијом урее. Врло специфична, шкољколика и ужаста, морфологија честица уочена је помоћу скенирајуће електронске микроскопије. Дифракција X-зрака показала је да је Eu^{3+}: CYS систем кристалисан у хексагоналној структурној решетки, карактеристичној за оксиапатит. У структури оксиапатита као домаћина, изведена је делимична замена Ca^{2+} и Y^{3+} јона са луминесцентно активним Eu^{3+} јонима чији су фотолуминесцентни спектри анализирани. Дата анализа указује на присуство Eu^{3+} јона на оба места, 4f са координацијом 9 и 6h са координацијом 7, показујући благи помак ка плавој области у поређењу са типичним спектром других итријум-силикатних фаза, као домаћина Eu^{3+} јона.*

Кључне речи*: рефлукс метода, еуропијумом допирани итријум оксиапатит, луминесцентне особине, кристална структура.*